INORGANIC CHEMISTRY

FRONTIERS

Accepted Manuscript

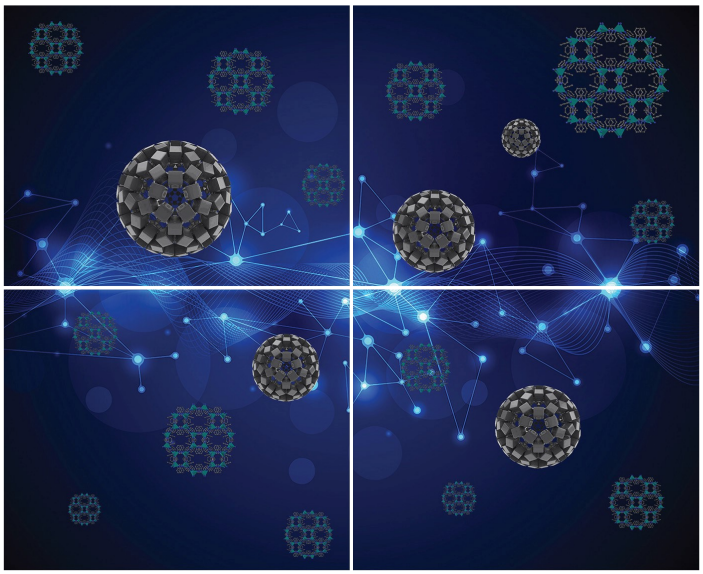

This article can be cited before page numbers have been issued, to do this please use: B. E. Osborne, C. Siakalli, R. Brown, A. J. P. White, C. Rocco, D. Weiss, E. Delgado, E. García-España, J. K. Sosabowski, M. Ma and N. J. Long, *Inorg. Chem. Front.*, 2026, DOI: 10.1039/D6QI01035K.

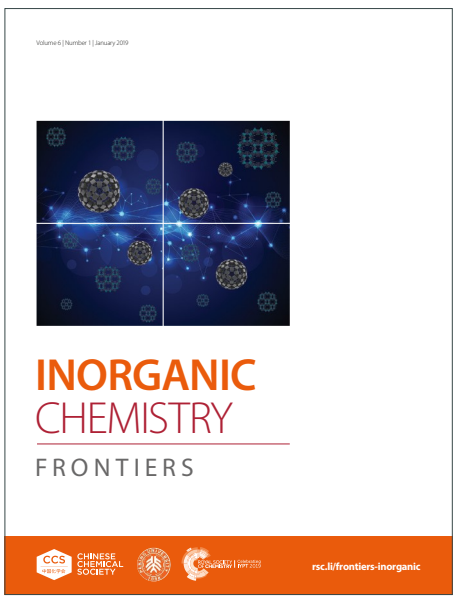

View Article Online
DOI: 10.1039/D6QI01035K

ARTICLE

Picolinamide-functionalized macrocyclic chelators for $^{203/212}$Pb theranostic radiotracers

Received 00th January 20xx,
Accepted 00th January 20xx

DOI: 10.1039/x0xx00000x

Bradley E. Osborne,*[a,b] Christina Siakalli,[a,b] Ryan K. Brown,[a] Andrew J. P. White,[a] Claudio Rocco,[c] Dominik Weiss,[c] Estefanía Delgado-Pinar,[d] Enrique García-España,[d] Jane K. Sosabowski,[e] Michelle T. Ma,[b] and Nicholas J. Long*[a]

Picolinamide-functionalized macrocyclic ligands represent a promising class of chelators for $^{203/212}$Pb-based theranostic applications, offering a dual role in both diagnostic imaging and targeted radiotherapy. In this study, two 18-membered diazacrown ligands, **K22_PicAm** and the novel **NPK_PicAm**, were synthesized and complexed with both non-radioactive Pb^{2+} and radiotherapeutic $^{212}Pb^{2+}$. Structural characterization via NMR spectroscopy and X-ray diffraction confirmed the formation of a single, highly rigid, symmetric **[Pb(K22_PicAm)]$^{2+}$** species. Density Functional Theory (DFT) and Natural Bond Orbital (NBO) analysis indicated stereochemically inactive $6s^2$ lone pairs in the Pb^{2+} complexes, leading to holodirected geometries. UV-vis spectroscopy and potentiometric titrations showed both ligands form highly stable Pb^{2+} complexes, with complete binding by **K22_PicAm** and **NPK_PicAm** between pH 4 and 9. Radiolabelling studies with ^{212}Pb demonstrated near-quantitative radiochemical conversion within 15 minutes. These results establish picolinamide-bearing macrocycles as promising candidates for the development of next-generation, targeted $^{203/212}$Pb theranostic agents and support their further exploration in radiopharmaceutical research.

Introduction

Lead(II)-based (Pb^{2+}) radiopharmaceuticals have gained significant interest in oncology due to their unique properties, offering a promising dual role in both diagnostic imaging and targeted radiotherapy.[1–3] Theranostic "look and treat" radiopharmaceuticals use pairs of radionuclides that are incorporated into the same or similar molecular architectures that target receptors selectively expressed on the surface of tumour cells. Indeed, these molecular pharmaceuticals have transformed treatment outcomes for many cancer patients, particularly in neuroendocrine and prostate cancer.[4,5] The first diagnostic radiopharmaceutical enables tumour imaging using either Positron (β^+) Emission Tomography (PET), or Single Photon Computed Tomography (SPECT), selecting patients who are eligible for the second, systemic therapeutic radiopharmaceutical, which emits cytotoxic alpha- (α), beta- (β^-), or Auger particles.[6–9] Either same-element isotope pairs ("true theranostics") or different-element isotope pairs can be employed.[10,11] For example, receptor-targeted peptide derivatives incorporating the PET radionuclide, gallium-68 (^{68}Ga, $t_{1/2}$ = 68 minutes) are used to stratify patients for companion receptor-targeted radiotherapies containing β^--emitting lutetium-177 (^{177}Lu, $t_{1/2}$ = 6.65 days).[12] Same-element isotope pairs, such as lead-203 (^{203}Pb, $t_{1/2}$ = 51.9 hours) and lead-212 (^{212}Pb, $t_{1/2}$ = 10.6 hours) are appealing as they enable a "true" molecular match, with the diagnostic agent having an identical chemical structure to the radiotherapeutic agent. ^{203}Pb is a suitable SPECT radionuclide; significantly, therapeutic ^{212}Pb emits both β^--particles, and an α-particle *via* the decay of its daughter nuclide bismuth-212 (^{212}Bi, $t_{1/2}$ = 60.6 minutes).[2,13–17] Preclinical studies with ^{203}Pb- and ^{212}Pb-based radiopharmaceuticals have demonstrated promising tumour targeting and therapeutic efficacy in pancreatic, melanoma, prostate, ovarian, and breast cancer models.[18–29] Notably, ^{212}Pb-radiopharmaceuticals are now advancing through early-phase clinical trials, showing favourable biodistribution and safety profiles in prostate, ovarian, and breast cancer.[30–35]

Chelators are critical to radiometal-based radiopharmaceuticals, as their resulting complexes need to possess sufficient thermodynamic and kinetic stability to deliver payload to diseased tissue *in vivo*.[36,37] DOTAM (TCMC, Fig. 1) is cited as the "gold-standard" for Pb^{2+}-based radiopharmaceuticals: its intermediate Lewis basic amides are more suitable for Pb^{2+} coordination compared to the analogous carboxylates of the prevalently used chelator, DOTA (Fig. 1).[36,38,39] Alongside DOTA and DOTAM, which are prevalently used in radiopharmaceuticals, several families of macrocyclic

[a] Department of Chemistry, Imperial College London, Molecular Sciences Research Hub, White City Campus, London, W12 0BZ, UK. E-mail: n.long@imperial.ac.uk and b.osborne18@imperial.ac.uk
[b] School of Biomedical Engineering and Imaging Sciences, King's College London, 4th Floor Lambeth Wing, St Thomas' Hospital, London, SE1 7EH, UK.
[c] Department of Earth Science and Engineering, Imperial College London, South Kensington Campus, London, SW7 2BP, UK.
[d] Institute of Molecular Sciences, Universitat de València, València, Spain.
[e] Centre for Cancer Biomarkers and Biotherapeutics, Barts Cancer Institute, Queen Mary University of London, London, UK.
† Footnotes relating to the title and/or authors should appear here.
Supplementary Information available: [details of any supplementary information available should be included here]. See DOI: 10.1039/x0xx00000x

View Article Online
DOI: 10.1039/D6QI01035K

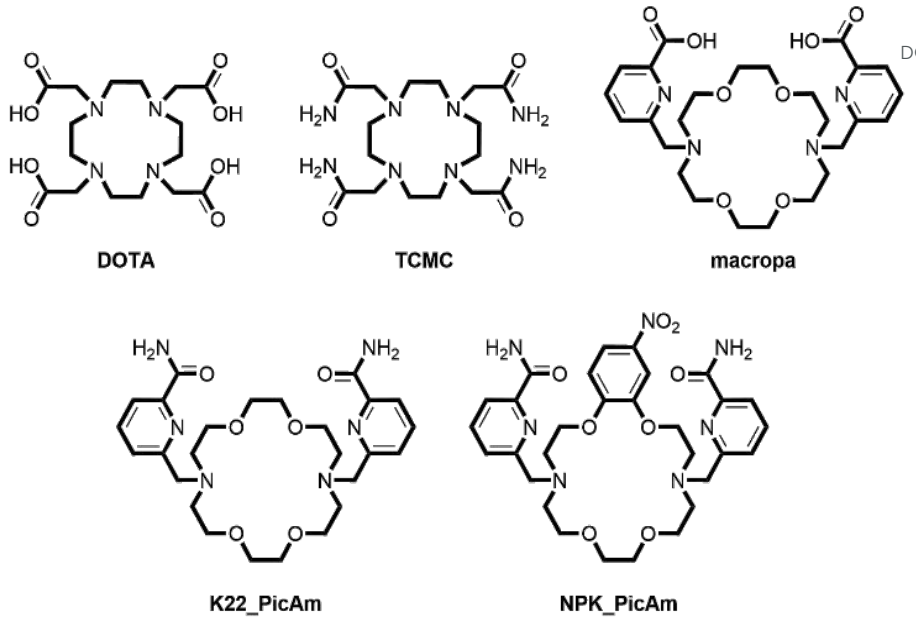

Figure 1. The structures of the chelators discussed in this work.

chelators have also been investigated for the complexation of Pb^{2+} radionuclides.[40–46] In particular, macropa (Fig. 1), an 18-membered macrocyclic chelator with picolinic acid pendant arms,[47] has demonstrated exceptional selectivity and radiochemical labelling efficiency with Pb^{2+}.[44,48] We hypothesized that substituting the picolinic acid pendant arms with picolinamide groups would further enhance the kinetic inertness and thermodynamic stability of the Pb^{2+} complexes. Although not yet reported for radiopharmaceutical purposes, **K22_PicAm** (Fig. 1) was first used for the complexation of Eu^{2+} to investigate its size-discrimination ability and redox stabilisation.[49] Here, we report the synthesis and characterisation of novel Pb^{2+} complexes of **K22_PicAm**, including a radiolabelled $^{212}Pb^{2+}$ complex. We additionally report a novel nitrophenyl analogue of **K22_PicAm**, **NPK_PicAm** (Scheme 1), as a potential precursor to enable functionalisation of **K22_PicAm** with biomolecules (e.g. peptides) for targeting receptors of cancer cells, via the nitrophenyl motif.[50]

Results and Discussion

Synthesis of the chelators

K22_PicAm was synthesised in 21 % yield from commercially available Kryptofix®22 by following a previously reported procedure[51] (Scheme 1). **NPK_PicAm** was synthesised in a similar manner to **K22_PicAm** in two steps. Refluxing compound **2**[52] in anhydrous acetonitrile with 2.1 equivalents of methyl 6-(chloromethyl)picolinate, and 4 equivalents of sodium carbonate gave compound **3** as an orange oil. **NPK_PicAm** was

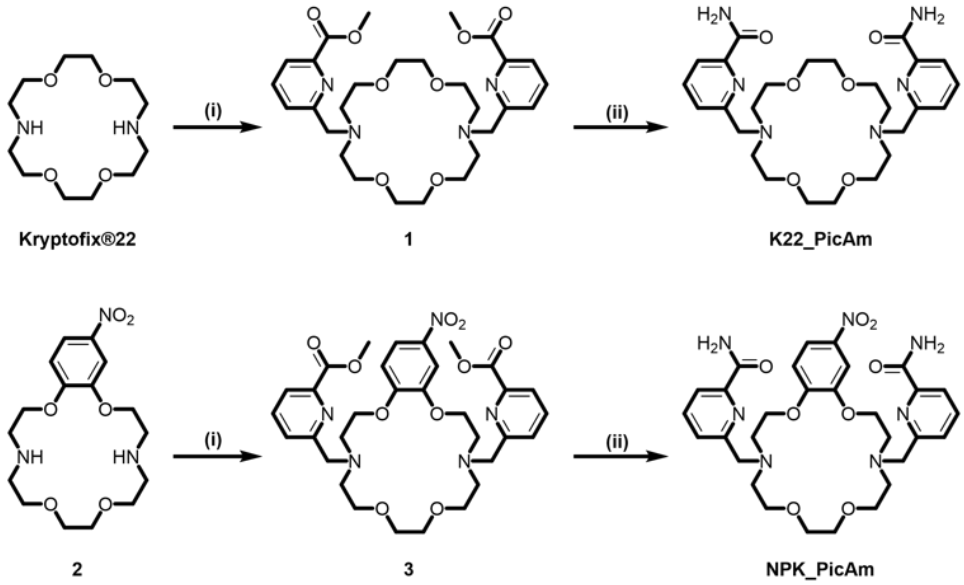

Scheme 1. The synthesis of chelators **K22_PicAm** and **NPK_PicAm**. Reaction conditions: (i) Methyl 6-(chloromethyl)picolinate, Na_2CO_3, MeCN, reflux, silica gel chromatography; (ii) $NH_{3(aq)}$ (35 % wt.), 0 to 25 °C, reverse-phase chromatography.

View Article Online
DOI: 10.1039/D6QI01035K

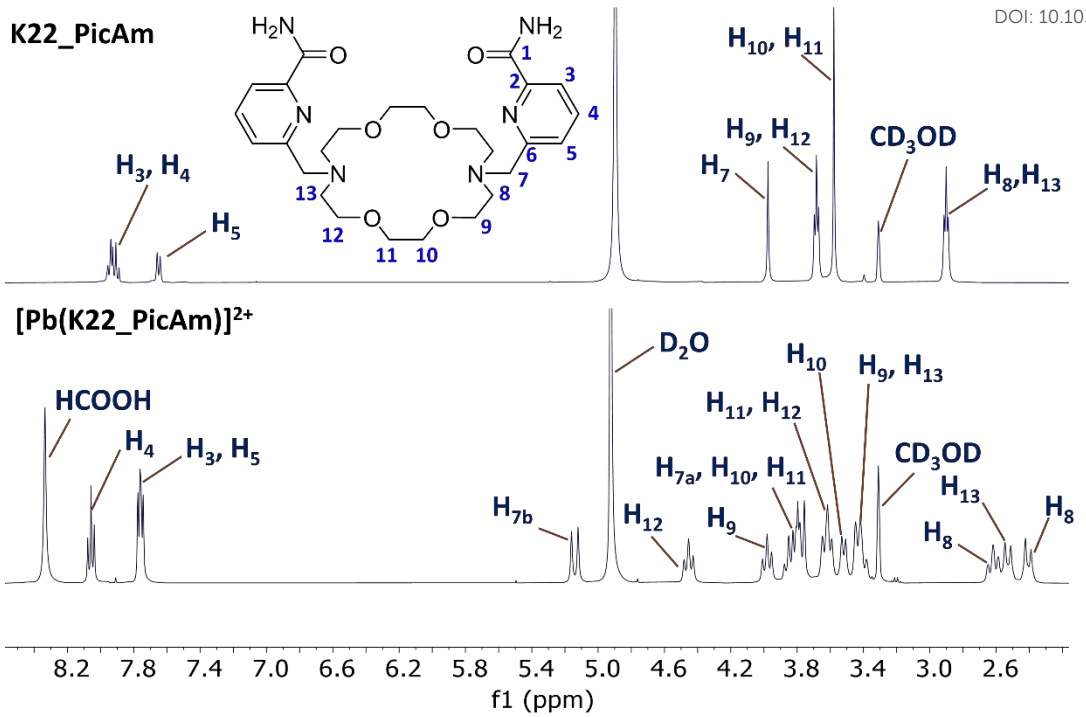

Figure 2. ^{1}H NMR spectra of **K22_PicAm**, and **[Pb(K22_PicAm)]$^{2+}$**, recorded in MeOD (400 MHz, 298 K).

obtained by aminolysis of **3,** as a yellow solid in 38 % yield after purification.

Solution-State Structures of Pb^{2+} Complexes

Pb^{2+} complexes were synthesised by the addition of 1.1 eq. of $Pb(OAc)_2 \bullet 3H_2O$ to a solution of the chelator in an aqueous NH_4OAc solution (pH 4.5) at room temperature. After stirring for 15 minutes, the mixture was purified via reverse-phase chromatography, and the desired complexes characterised via NMR and MS (Fig. S13-S17, Fig. S19-S20, and Fig. S24-S25, ESI). These complexation conditions were repeated in MeOD to record the complete reaction system and to assess the behaviour of the Pb^{2+} complexes in solution (Fig. 2). The ^{1}H NMR spectrum of **[Pb(K22_PicAm)]$^{2+}$** is characteristic of a single highly rigid C_2 symmetric species, evidenced by the presence of well-resolved aliphatic proton resonances, in contrast to other polyether complexes which are known to exhibit dynamic and fluxional behaviour.[43,53] Further, geminal AB type splitting patterns are observed for all methylene and ethylene protons in the Pb^{2+} complex. The presence of a single, highly rigid species suggests that this complex could possess the requisite stability that is critical for *in vivo* applications. The ^{207}Pb NMR spectrum of the complex **[Pb(K22_PicAm)]$^{2+}$** displays a single signal at — 2289 ppm (Fig. 3 and Fig. S19, ESI), versus $Pb(NO_3)_2$, which is within the range of macrocyclic crown systems with carboxylic acid and amide pendant arms reported previously (— 2076 to — 2299 ppm).[40,41] Pb^{2+} complexation experiments with **NPK_PicAm** were undertaken by reacting 1 eq. of Pb^{2+} with 1 eq. of **NPK_PicAm** at 25 °C. ^{1}H NMR, HRMS (ES-TOF+) and HPLC analyses (Fig. S20, Fig. S25 and Fig. S29-S30, ESI) indicated the formation of a single product, consistent with the formation of **[Pb(NPK_PicAm)]$^{2+}$**. The ^{1}H NMR spectrum of **[Pb(NPK_PicAm)]$^{2+}$** was more complex than that of **[Pb(K22_PicAm)]$^{2+}$** (Fig. 2) due to the relative lower symmetry of the former, which arises from the incorporation of a nitrophenyl group. However, compared to **[Pb(K22_PicAm)]$^{2+}$**, similar patterns in chemical shift changes were observed upon coordination of **NPK_PicAm** to Pb^{2+}. HRMS (ES-TOF+) analysis showed the expected *m/z* signals for a complex of formula **[Pb(NPK_PicAm)]$^{2+}$**. HPLC analysis showed the formation of a single Pb-bound species, with a retention time distinct to that of the free ligand.

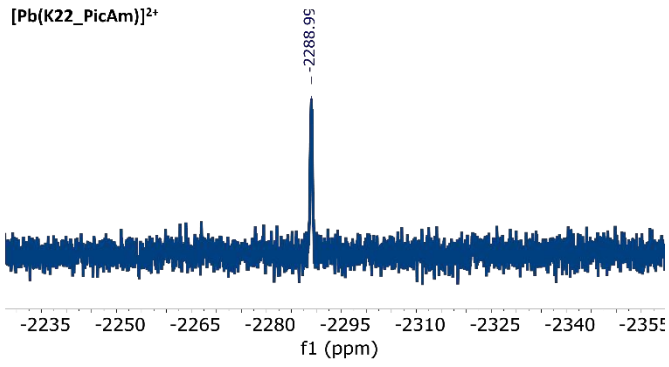

Figure 3. ^{207}Pb{^{1}H} NMR spectrum of **[Pb(K22_PicAm)]$^{2+}$**, recorded in D_2O (84 MHz, 298 K).

X-Ray Crystal Structure of the [Pb(K22_PicAm)]$^{2+}$ Complex

Single crystals of **[Pb(K22_PicAm)]-2PF_6** suitable for X-ray diffraction studies (Fig. 4, Fig. S41 and Table S2, ESI) were obtained. Bond distances and angles of the Pb^{2+} coordination environments are listed in Table 1 and Table S3, ESI. Compound **[Pb(K22_PicAm)]-2PF_6** crystallizes in the tetragonal *I4/m* space group, with the crystal containing two non-coordinated PF_6^-

View Article Online
DOI: 10.1039/D6QI01075K

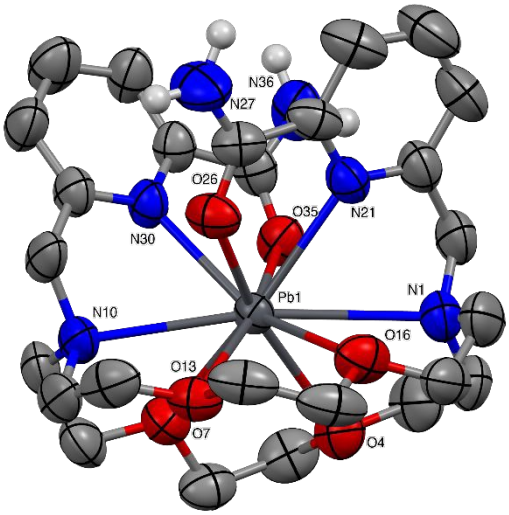

Figure 4. The structure of the cationic complex present in the crystal of **[Pb(K22_PicAm)]-2PF$_6$**. Thermal ellipsoids are drawn at the 50 % probability level. Hydrogen atoms and both PF_6 anions are omitted for clarity.

anions. The Pb^{2+} metal ion in **[Pb(K22_PicAm)]-2PF$_6$** is ten-coordinated by the chelator, which binds through the two N and four O donor atoms of the macrocycle, two pyridyl N atoms, and two amide O atoms.[47] The macrocyclic Pb-N and Pb-O distances (Table 1 and Table S3, ESI) range from 2.89 to 3.05 Å, whereas pyridyl Pb-N distances (2.61 to 2.68 Å) are shorter. Amide Pb-O distances are shorter again (2.53 to 2.60 Å). The structure of **[Pb(K22_PicAm)]-2PF$_6$** displays shorter bond lengths involving donor atoms of the picolinamide pendant arms, whereas the donor atoms of the macrocyclic unit fall within a longer bond length range. This indicates that the donor atoms of the picolinamide pendant arms provide the strongest interactions with the Pb^{2+} ion. A similar trend in bond lengths was reported

Table 1. Bonding distances (Å) of the Pb^{2+} coordination environments in the X-ray structure of **[Pb(K22_PicAm)]-2PF$_6$** shown in **Fig. 4**.

	[Pb(K22_PicAm)]-2PF$_6$
Pb(1)-O(26)	2.534(4)
Pb(1)-O(35)	2.604(4)
Pb(1)-N(30)	2.613(5)
Pb(1)-N(21)	2.679(5)
Pb(1)-N(10)	2.890(5)
Pb(1)-O(7)	2.891(4)
Pb(1)-O(16)	2.910(4)
Pb(1)-O(13)	2.925(4)
Pb(1)-O(4)	3.015(4)
Pb(1)-N(1)	3.045(5)

for the Pb^{2+} complex of macropa, in which the shortest bonds were observed between picolinate N and O donor atoms and Pb, with longer bond distances – similar to those observed here for **[Pb(K22_PicAm)]-2PF$_6$** – reported between macrocyclic N and O donors and Pb.[47,48] An alternative trend in coordination of Pb^{2+} to multidentate macrocyclic chelators has also been reported, in which donor atoms of the macrocycle form stronger interactions with the Pb^{2+} metal ion compared to donor atoms of the pendant arms. This type of coordination has been observed in the Pb^{2+} complexes of the cyclen derivatives DOTA, DOTAM and THP-12-ane-N_4, along with other azacrown macrocycles,[39,41,54–56] although these structures are all considered to be hemidirected.

DFT Calculations

Having the electronic configuration [Xe]$4f^{14}5d^{10}6s^2$, Pb^{2+} is one of the post-transition metal elements that exhibits the "inert pair effect".[57] The resulting lone pair of electrons are stereochemically active or inactive. Such Pb^{2+} complexes are termed as holodirected (inactive lone pair, even donor atom distribution) or hemidirected (active lone pair, uneven distribution of donor atoms), with the latter exhibiting lower stability under certain conditions.[58] Hemidirected complexes are favoured by low coordination numbers, and hard and charged donor atoms, whereas holodirected complexes prefer high coordination numbers and soft donor atoms.[59] Natural Bond Orbital (NBO) analysis can quantify the $6s^2$ lone pair character of Pb^{2+} complexes by analysing electron density distribution, orbital interactions, and hybridisation. If the lone pair has significant s-character with minimal 6p orbital mixing, it is likely to be stereochemically inactive, favouring holodirected geometry. Using DFT, NBO analysis of **[Pb(K22_PicAm)]$^{2+}$** and **[Pb(NPK_PicAm)]$^{2+}$** indicates that the Pb^{2+} lone pair is stereochemically inactive in both complexes due to the insignificant 6p contribution (0.59 % and 0.60 % respectively) to the $6s^2$ lone pair (Fig. S42-S45 and Table S5-S6, ESI), signifying both complexes are holodirected. Initial geometries for **K22_PicAm** and **NPK_PicAm** and their respective Pb^{2+} complexes were taken from the crystal structure of macropa with modification of picolinate arms to picolinamide arms and the addition of a nitrophenyl group in the macrocyclic ring.[48] The optimized structures of the Pb^{2+} complexes are consistent with the X-ray crystal structure **[Pb(K22_PicAm)]-2PF$_6$** in which there is no distinct void in the Pb^{2+} coordination sphere, indicative of a stereochemically inactive lone pair, supporting the presence of a holodirected complex.

Protonation Constants and Thermodynamic Stability of the Pb^{2+} Complexes

To investigate the properties and affinity of the new ligands for Pb^{2+}, potentiometry and UV-Vis spectroscopy were used to determine the protonation constants (K_i) and the Pb^{2+} stability constants (K_{PbL}) (Table 2). Consistent with previous reports,[49] we find that potentiometric measurements resolve only two protonation constants for the systems studied. The second protonation constant (log K_{H2}) determined in this study is in good agreement with literature values, while some variation is observed for the first constant (log K_{H1}), which we attribute to

View Article Online
DOI: 10.1039/D6QI01035K

Table 2. Protonation and Pb^{2+} complex formation constants for the ligands **K22_PicAm** and **NPK_PicAm** (L). (a) Determined by potentiometric titration in 0.15 M NaCl at 25 °C in this study; (b) determined from spectroscopic titration data and using protonation constants obtained in this study; (c) determined by potentiometric titration in 0.1 M KCl at 25 °C in a study reported by Regueiro-Figueroa *et al*;[49] and (d) calculated from spectroscopic titration data obtained in this study and using protonation constants reported in the literature.[49] **pPb** corresponds to the negative logarithm of the equilibrium concentration of uncomplexed Pb^{2+} in the presence of the ligand at pH 7.4.

	Reaction	K22_PicAm		NPK_PicAm
Log K_{H1}	$H^+ + L \leftrightarrows HL^+$	7.90(2)[a]	7.08[c]	7.82(1)[a]
Log K_{H2}	$H^+ + HL^+ \leftrightarrows H_2L^{2+}$	6.43(1)[a]	6.40[c]	5.422(7)[a]
Log K_{PbL}	$Pb^{2+} + L \leftrightarrows [PbL]^{2+}$	14.19(2)[b]	13.28[d]	11.68(4)[a]
Log K_{PbLOH}	$Pb^{2+} + L \leftrightarrows [PbL(OH)]^+ + H^+$			0.97(4)[a]
pPb		14.5	14.0	12.1

differences in ionic strength and electrolyte. Comparison with the **NPK_PicAm**, for which potentiometric measurements provided well-defined constants (Table 2), supports the assigned value for the first protonation constant of **K22_PicAm** (log K_{H1} = 8.30). The observed UV-Vis absorption spectra suggest the presence of two different protonation processes. At acidic pH, the absorption spectrum displays a band centred at 270 nm, with shoulders at 262 and 276 nm. Upon gradual addition of NaOH(aq), the band broadens slightly and absorbance decreases until pH 5.6, followed by an increase in absorbance until pH 9.0, when a plateau is reached (Fig. S37, ESI). The decrease in absorbance in acidic pH might correspond to the deprotonation of the pyridine nitrogen atoms while the increase in absorption correspond possibly to deprotonation of the tertiary ammonium groups of the macrocycle.[60] While our observed UV-Vis trends are consistent with multiple protonation sites, the combined spectroscopic, potentiometric and literature data support a model in which the dominant observable equilibria correspond to the tertiary amine groups of the macrocyclic ring.[41,54]

Potentiometric measurements indicate that complex formation occurs predominantly in a pH range where competition from protons is minimal, making the extraction of reliable stability constants (log K_{PbL}) from these data challenging. Therefore, spectroscopic titrations were performed using solutions containing Pb^{2+} and **K22_PicAm** in a 0.9:1.0 molar ratio, titrated with aqueous NaOH starting from pH < 2 (Fig. S38, ESI). Pb^{2+} complex formation is observed at low pH (approx. 2, see Fig. S38, ESI). Absorption at 276 nm increases progressively with a maximum at pH 3.6, indicating quantitative formation of **[Pb(K22_PicAm)]$^{2+}$** ($[PbL]^{2+}$). At pH above 10, absorbance slightly increases suggesting the formation of a minor hydroxide species $[PbL(OH)]^+$. To determine the stability constant for the Pb-L complexes, a chemical model was developed using protonation constants derived from potentiometric measurements conducted during this study and a previous study.[49] The spectrophotometric experimental titration data was fitted using the software program HypSpec.[61] We find for the formation of a $[PbL]^{2+}$ species log K_{PbL} values ranging from

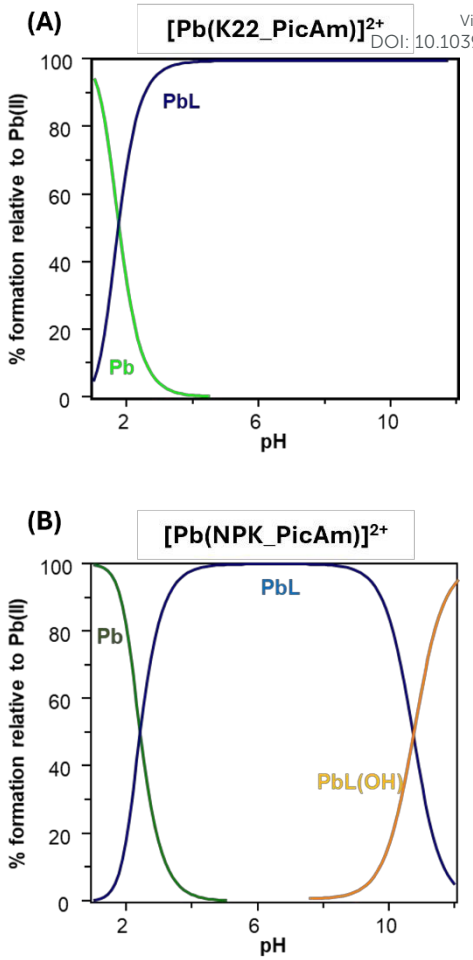

Figure 5. Speciation diagrams of the system Pb^{2+}-L. A) **K22_PicAm;** B) **NPK_PicAm**

13.28 to 14.19, indicating quantitative complexation of lead at pH 7.4.

Both ligands achieve quantitative Pb^{2+} binding under mildly acidic conditions (pH 3-5) and **K22_PicAm** exhibits a higher apparent stability compared to **NPK_PicAm** and pPb for **NPK_PicAm** is two logarithmic units lower.

The incorporation of a rigidifying and electron-withdrawing nitrophenyl group into the macrocyclic backbone results in an expected decrease in thermodynamic stability. The speciation diagrams (Fig. 5) indicate that under the conditions tested here, all Pb^{2+} in solution is bound to the chelator, either **K22_PicAm** and **NPK_PicAm**, above pH ≈ 4 and below pH ≈ 9. Notably, this pH range is well aligned with conditions commonly employed for $^{203}Pb/^{212}Pb$ radiolabelling, and the efficient complex formation observed in this work is consistent with the results shown in the ^{212}Pb labelling discussed below.

Lead-212 Radiolabelling Studies

Radiolabelling reactions of **K22_PicAm** and **NPK_PicAm** with $[^{212}Pb]Pb^{2+}$ were undertaken. In these reactions, a solution of $[^{212}Pb]Pb(OAc)_2$ (~1 MBq) was added to a solution of chelator and reacted for 15 minutes at either 37 °C or 95 °C, with the final reaction containing the pertinent chelator at a concentration of 1 mM, 100 µM, 50 µM, 10 µM or 5 µM, at pH 5.5, in 0.5 M NaOAc buffer. Radiochemical conversions (RCCs) were assessed using radio-iTLC and are summarised in Table S1,

ESI. Upon heating at 95 °C for 15 minutes, **K22_PicAm** produced near quantitative RCCs across all chelator concentrations (Fig. 6A). At 37 °C, and a chelator concentration of 100 µM, a RCY of 88 % was achieved, and at a chelator concentration of 10 µM a RCC of 66 % was achieved. Comparatively, for **NPK_PicAm** a steady decrease in RCC values was observed as the chelator concentration was decreased (Fig. 6B). At a chelator concentration of 1 mM (10^{-3} M), **NPK_PicAm** achieved a RCC value of 85 %, whereas at a lower chelator concentration of 5 µM (5×10^{-6} M) a RCC value of 23 % was achieved. Due to the lower RCC observed for **NPK_PicAm** at high temperature, we did not investigate $[^{212}Pb]Pb^{2+}$ labelling with **NPK_PicAm** at lower temperatures. These preliminary findings underscore the potential of the **K22_PicAm** ligand system as a foundation for developing Pb^{2+}-based bifunctional chelators, paving the way for future structural refinements tailored to a broad spectrum of biological targeting vectors.

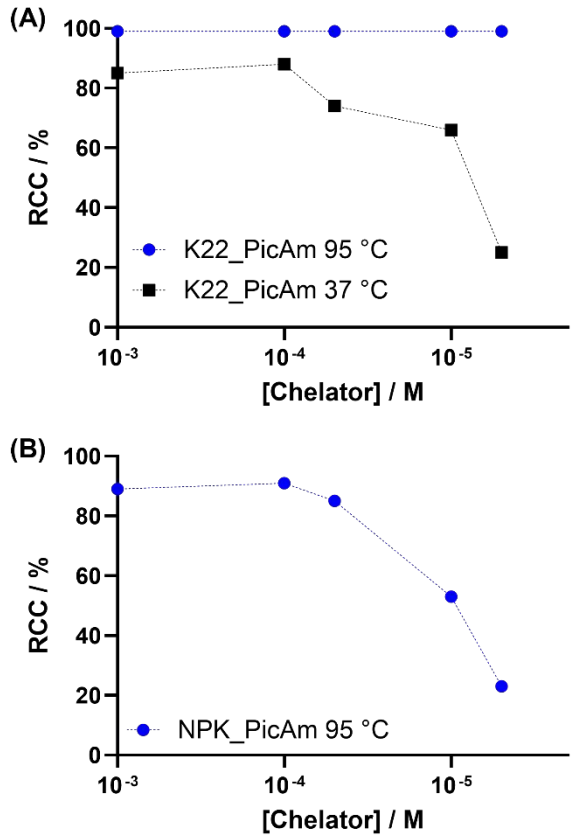

Figure 6. The radiochemical conversion (RCC) values for $[^{212}Pb]Pb^{2+}$ labelling with **(A) K22_PicAm** at chelator concentrations 1 mM to 5 µM over 15 minutes at 37 °C and 95 °C, and **(B) NPK_PicAm** at chelator concentrations 1 mM to 5 µM over 15 minutes at 95 °C.

Conclusions

In summary, we report two 18-membered diazacrown macrocyclic chelators bearing picolinamide pendant arms, **K22_PicAm** and **NPK_PicAm** for ^{212}Pb radiopharmaceuticals. Structural NMR and X-ray diffraction studies show that **[Pb(K22_PicAm)]$^{2+}$** forms a single, highly rigid, symmetric species, and UV-Vis spectrophotometric and potentiometric titrations showed that both **K22_PicAm** and **NPK_PicAm** form highly stable Pb^{2+} complexes. Radiolabelling each of these chelators with $^{212}Pb^{2+}$ achieved near-quantitative radiochemical conversion within 15 minutes at high temperatures.

As metallic radionuclides, such as ^{212}Pb, with therapeutically efficacious decay profiles become available for clinical application, chelator technologies such as **K22_PicAm** and **NPK_PicAm** are critical to enable their therapeutic application, to benefit patients. Recent first-in-human translational studies of radiotherapeutic ^{212}Pb agents highlight the significant potential of **K22_PicAm** and **NPK_PicAm** chelators as chemical platforms for the development of $^{203/212}Pb$-based theranostic agents. Further functionalisation of these chelators with receptor-targeted motifs will transform the **K22_PicAm** scaffold into a precision-guided tool for application as a molecular theranostic agent in combination with lead radionuclides.

Author contributions

BEO synthesised the compounds, performed the analyses, carried out the radiolabelling, and DFT calculations. X-ray crystallography was performed by RKB. Potentiometric titrations were performed by CS. UV-Vis spectrophotometric titrations were performed by ED-P and EG-E. MTM and NJL supervised the project, and all the authors contributed to the writing of the manuscript.

Conflicts of interest

There are no conflicts to declare.

Data availability

The data supporting this article have been included as part of the ESI. CCDC 2432138 contains the supplementary crystallographic data for **[Pb(K22_PicAm)]$^{2+}$**. The data can be obtained free of charge via www.ccdc.cam.ac.uk/data_request/cif, or by emailing data_request@ccdc.cam.ac.uk, or by contacting The Cambridge Crystallographic Data Centre, 12 Union Road, Cambridge CB2 1EZ, UK; fax: +44 1223 336033.

Acknowledgements

This research was supported by the EPSRC programme for Next Generation Molecular Imaging and Therapy with Radionuclides (EP/S019901/1, "MITHRAS") and Cancer Research UK (C63178/A24959).

Notes and references

1 J. C. dos Santos, M. Schäfer, U. Bauder-Wüst, W. Lehnert, K. Leotta, A. Morgenstern, K. Kopka, U. Haberkorn, W. Mier and C. Kratochwil, Development and dosimetry of $^{203}Pb/^{212}Pb$-labelled PSMA ligands: bringing "the lead" into

PSMA-targeted alpha therapy?, *Eur. J. Nucl. Med. Mol. Imaging*, 2019, **46**, 1081–1091.

2 R. G. Li, V. Y. Stenberg and R. H. Larsen, An Experimental Generator for Production of High-Purity ^{212}Pb for Use in Radiopharmaceuticals, *J. Nucl. Med.*, 2023, **64**, 173–176.

3 H. S. Chong, H. A. Song, X. Ma, D. E. Milenic, E. D. Brady, S. Lim, H. Lee, K. Baidoo, D. Cheng and M. W. Brechbiel, Novel bimodal bifunctional ligands for radioimmunotherapy and targeted MRI, *Bioconjug. Chem.*, 2008, **19**, 1439–1447.

4 J. Strosberg, G. El-Haddad, E. Wolin, A. Hendifar, J. Yao, B. Chasen, E. Mittra, P. L. Kunz, M. H. Kulke, H. Jacene, D. Bushnell, T. M. O'Dorisio, R. P. Baum, H. R. Kulkarni, M. Caplin, R. Lebtahi, T. Hobday, E. Delpassand, E. Van Cutsem, A. Benson, R. Srirajaskanthan, M. Pavel, J. Mora, J. Berlin, E. Grande, N. Reed, E. Seregni, K. Öberg, M. Lopera Sierra, P. Santoro, T. Thevenet, J. L. Erion, P. Ruszniewski, D. Kwekkeboom and E. Krenning, Phase 3 Trial of ^{177} Lu-Dotatate for Midgut Neuroendocrine Tumors, *New England Journal of Medicine*, 2017, **376**, 125–135.

5 O. Sartor, J. de Bono, K. N. Chi, K. Fizazi, K. Herrmann, K. Rahbar, S. T. Tagawa, L. T. Nordquist, N. Vaishampayan, G. El-Haddad, C. H. Park, T. M. Beer, A. Armour, W. J. Pérez-Contreras, M. DeSilvio, E. Kpamegan, G. Gericke, R. A. Messmann, M. J. Morris and B. J. Krause, Lutetium-177–PSMA-617 for Metastatic Castration-Resistant Prostate Cancer, *New England Journal of Medicine*, 2021, **385**, 1091–1103.

6 T. I. Kostelnik and C. Orvig, Radioactive Main Group and Rare Earth Metals for Imaging and Therapy, *Chem. Rev.*, 2019, **119**, 902–956.

7 S. L. Pimlott and A. Sutherland, Molecular tracers for the PET and SPECT imaging of disease, *Chem. Soc. Rev.*, 2010, **40**, 149–162.

8 D. E. Milenic and M. W. Brechbiel, Targeting of Radio-Isotopes for Cancer Therapy, *Cancer Biol. Ther.*, 2004, **3**, 361–370.

9 L. Filippi, A. Chiaravalloti, O. Schillaci, R. Cianni and O. Bagni, Theranostic approaches in nuclear medicine: current status and future prospects, *Expert Rev. Med. Devices*, 2020, **17**, 331–343.

10 N. H. Álvarez, D. Bauer, J. Hernández-Gil and J. S. Lewis, Recent Advances in Radiometals for Combined Imaging and Therapy in Cancer, *ChemMedChem*, 2021, **16**, 2909–2941.

11 C. Miller, J. Rousseau, C. F. Ramogida, A. Celler, A. Rahmim and C. F. Uribe, Implications of physics, chemistry and biology for dosimetry calculations using theranostic pairs, *Theranostics*, 2022, **12**, 232–259.

12 S. R. Banerjee, V. Kumar, A. Lisok, J. Chen, I. Minn, M. Brummet, S. Boinapally, M. Cole, E. Ngen, B. Wharram, C. Brayton, R. F. Hobbs and M. G. Pomper, ^{177}Lu-labeled low-molecular-weight agents for PSMA-targeted radiopharmaceutical therapy, *Eur. J. Nucl. Med. Mol. Imaging*, 2019, **46**, 2545–2557.

13 B. L. McNeil, A. K. H. Robertson, W. Fu, H. Yang, C. Hoehr, C. F. Ramogida and P. Schaffer, Production, purification, and radiolabeling of the ^{203}Pb/^{212}Pb theranostic pair, *EJNMMI Radiopharm. Chem.*, 2021, **6**, 6.

14 T. Rold, N. Okoye, E. Devanny, A. Berendzen, T. Dresser, T. Quinn and T. Hoffman, Pb-203/Pb-212 Evaluation as Theranostic Pair for Prostate Cancer Detection, Monitoring, and Treatment, *J. Nucl. Med.*, 2020, **61**, 229–229.

15 D. Máthé, K. Szigeti, N. Hegedus, I. Horváth, D. S. Veres, B. Kovács and Z. Szucs, Production and in vivo imaging of ^{203}Pb as a surrogate isotope for *in vivo* ^{212}Pb internal absorbed dose studies, *Applied Radiation and Isotopes*, 2016, **114**, 1–6.

16 K. Yong and M. W. Brechbiel, Towards translation of ^{212}Pb as a clinical therapeutic; getting the lead in!, *Dalton Trans.*, 2011, **40**, 6068–6076.

17 B. J. B. Nelson, J. Wilson, M. K. Schultz, J. D. Andersson and F. Wuest, High-yield cyclotron production of ^{203}Pb using a sealed ^{205}Tl solid target, *Nucl. Med. Biol.*, 2023, **116–117**, 108314.

18 L. L. Chappell, E. Dadachova, D. E. Milenic, K. Garmestani, C. Wu and M. W. Brechbiel, Synthesis, characterization, and evaluation of a novel bifunctional chelating agent for the lead isotopes ^{203}Pb and ^{212}Pb, *Nucl. Med. Biol.*, 2000, **27**, 93–100.

19 V. Boudousq, L. Bobyk, M. Busson, V. Garambois, M. Jarlier, P. Charalambatou, A. Pèlegrin, S. Paillas, N. Chouin, F. Quenet, P. Maquaire, J. Torgue, I. Navarro-Teulon and J.-P. Pouget, Comparison between Internalizing Anti-HER2 mAbs and Non-Internalizing Anti-CEA mAbs in Alpha-Radioimmunotherapy of Small Volume Peritoneal Carcinomatosis Using ^{212}Pb, *PLoS One*, 2013, **8**, e69613.

20 Y. Miao, M. Hylarides, D. R. Fisher, T. Shelton, H. Moore, D. W. Wester, A. R. Fritzberg, C. T. Winkelmann, T. Hoffman and T. P. Quinn, Melanoma Therapy via Peptide-Targeted

α-Radiation, *Clinical Cancer Research*, 2005, **11**, 5616–5621.

21 Y. Miao, S. D. Figueroa, D. R. Fisher, H. A. Moore, R. F. Testa, T. J. Hoffman and T. P. Quinn, ^{203}Pb-Labeled α-Melanocyte–Stimulating Hormone Peptide as an Imaging Probe for Melanoma Detection, *Journal of Nuclear Medicine*, 2008, **49**, 823.

22 J. Yang, J. Xu, L. Cheuy, R. Gonzalez, D. R. Fisher and Y. Miao, Evaluation of a Novel Pb-203-Labeled Lactam-Cyclized Alpha-Melanocyte-Stimulating Hormone Peptide for Melanoma Targeting, *Mol. Pharm.*, 2019, **16**, 1694–1702.

23 T. A. R. Stallons, A. Saidi, I. Tworowska, E. S. Delpassand and J. J. Torgue, Preclinical Investigation of ^{212}Pb-DOTAMTATE for Peptide Receptor Radionuclide Therapy in a Neuroendocrine Tumor Model, *Mol. Cancer Ther.*, 2019, **18**, 1012–1021.

24 B. Kasten, J. Fan, S. Ferrone, K. Zinn and D. Buchsbaum, Targeted radioimmunotherapy of triple negative breast cancer with CSPG4-specific ^{212}Pb-labeled monoclonal antibody., *Journal of Nuclear Medicine*, 2016, **57**, 114.

25 B. Kasten, J. Fan, S. Ferrone, K. Zinn and D. Buchsbaum, Targeted radioimmunotherapy of triple negative breast cancer with CSPG4-specific ^{212}Pb-labeled monoclonal antibody., *Journal of Nuclear Medicine*, 2016, **57**, 114.

26 B. B. Kasten, A. Gangrade, H. Kim, J. Fan, S. Ferrone, C. R. Ferrone, K. R. Zinn and D. J. Buchsbaum, ^{212}Pb-labeled B7-H3-targeting antibody for pancreatic cancer therapy in mouse models, *Nucl. Med. Biol.*, 2018, **58**, 67–73.

27 B. B. Kasten, R. C. Arend, A. A. Katre, H. Kim, J. Fan, S. Ferrone, K. R. Zinn and D. J. Buchsbaum, B7-H3-targeted ^{212}Pb radioimmunotherapy of ovarian cancer in preclinical models, *Nucl. Med. Biol.*, 2017, **47**, 23–30.

28 I. Quelven, J. Monteil, M. Sage, A. Saidi, J. Mounier, A. Bayout, J. Garrier, M. Cogne and S. Durand-Panteix, ^{212}Pb α-Radioimmunotherapy Targeting CD38 in Multiple Myeloma: A Preclinical Study, *Journal of Nuclear Medicine*, 2020, **61**, 1058.

29 M. Li, D. Liu, D. Lee, S. Kapoor, K. N. Gibson-Corley, T. P. Quinn, E. A. Sagastume, S. L. Mott, S. A. Walsh, M. R. Acevedo, F. L. Johnson and M. K. Schultz, Enhancing the Efficacy of Melanocortin 1 Receptor-Targeted Radiotherapy by Pharmacologically Upregulating the Receptor in Metastatic Melanoma, *Mol. Pharm.*, 2019, **16**, 3904–3915.

30 R. F. Meredith, J. J. Torgue, T. A. Rozgaja, E. P. Banaga, P. W. Bunch, R. D. Alvarez, J. M. J. Straughn, M. C. Dobelbower and A. M. Lowy, Safety and Outcome Measures of First-in-Human Intraperitoneal α Radioimmunotherapy With ^{212}Pb-TCMC-Trastuzumab, *Am. J. Clin. Oncol.*

31 R. Meredith, J. Torgue, S. Shen, D. R. Fisher, E. Banaga, P. Bunch, D. Morgan, J. Fan and J. M. Straughn, Dose Escalation and Dosimetry of First-in-Human α Radioimmunotherapy with ^{212}Pb-TCMC-Trastuzumab, *Journal of Nuclear Medicine*, 2014, **55**, 1636.

32 R. F. Meredith, J. Torgue, M. T. Azure, S. Shen, S. Saddekni, E. Banaga, R. Carlise, P. Bunch, D. Yoder and R. Alvarez, Pharmacokinetics and Imaging of ^{212}Pb-TCMC-Trastuzumab After Intraperitoneal Administration in Ovarian Cancer Patients, *Cancer Biother. Radiopharm.*, 2013, **29**, 12–17.

33 E. S. Delpassand, I. Tworowska, R. Esfandiari, J. Torgue, J. Hurt, A. Shafie and R. Núñez, Targeted α-Emitter Therapy with ^{212}Pb-DOTAMTATE for the Treatment of Metastatic SSTR-Expressing Neuroendocrine Tumors: First-in-Humans Dose-Escalation Clinical Trial, *J. Nucl. Med.*, 2022, **63**, 1326–1333.

34 M. R. Griffiths, D. A. Pattison, M. Latter, K. Kuan, S. Taylor, W. Tieu, T. Kryza, D. Meyrick, B. Q. Lee, A. Hansen, S. E. Rose and S. G. Puttick, First-in-Human ^{212}Pb-PSMA–Targeted α-Therapy SPECT/CT Imaging in a Patient with Metastatic Castration-Resistant Prostate Cancer, *Journal of Nuclear Medicine*, 2024, **65(4)**, 664.

35 K. Berner, E. Hernes, M. Kvassheim, M.-E. Revheim, J. Bastiansen, S. Selboe, C. L. Bakken, S. R. Grønningsæter, Ø. S. Bruland, R. H. Larsen, L. Bouzelmat, V. L. Jardine and C. Stokke, First-in-Human Phase 0 Study of AB001, a Prostate-Specific Membrane Antigen–Targeted ^{212}Pb Radioligand, in Patients with Metastatic Castration-Resistant Prostate Cancer, *Journal of Nuclear Medicine*, 2025, **66(5)**, 732-738.

36 E. W. Price and C. Orvig, Matching chelators to radiometals for radiopharmaceuticals, *Chem. Soc. Rev.*, 2014, **43**, 260–290.

37 M. W. Brechbiel, Bifunctional Chelates for Metal Nuclides, *Q. J. Nucl. Med. Mol. Imaging*, 2008, **52**, 166–173.

38 R. G. Pearson, Hard and Soft Acids and Bases, *J. Am. Chem. Soc.*, 1963, **85**, 3533–3539.

39 R. D. Hancock, J. H. Reibenspies and H. Maumela, Structural Effects of the Lone Pair on Lead(II), and Parallels with the Coordination Geometry of Mercury(II). Does the Lone Pair on Lead(II) Form H-Bonds? Structures of the Lead(II) and Mercury(II) Complexes of the Pendant-Donor

Macrocycle DOTAM (1,4,7,10-Tetrakis(carbamoylmethyl)-1,4,7,10-tetraazacyclododecane), *Inorg. Chem.*, 2004, **43**, 2981–2987.

40 C. Harriswangler, B. L. McNeil, I. Brandariz, L. Valencia, D. Esteban-Gómez, C. F. Ramogida and C. Platas-Iglesias, Incorporation of Carboxylate Pendant Arms into 18-Membered Macrocycles: Effects on [$^{nat/203}$ Pb]Pb(II) Complexation, *Chemistry – A European Journal*, 2024, **30**, e202400434.

41 C. Harriswangler, B. L. McNeil, I. Brandariz-Lendoiro, F. Lucio-Martínez, L. Valencia, D. Esteban-Gómez, C. F. Ramogida and C. Platas-Iglesias, Exploring the use of rigid 18-membered macrocycles with amide pendant arms for Pb(II)-based radiopharmaceuticals, *Inorg. Chem. Front.*, 2024, **11**, 1070–1086.

42 M. L. Grieve, P. R. W. J. Davey, P. V. Bernhardt, C. M. Forsyth and B. M. Paterson, Rapid and stable complexation of the α-generators bismuth-212 and lead-212 with a tetraazamacrocyclic chelator bearing thiosemicarbazone pendant arms, *Inorg. Chem. Front.*, 2024.

43 B. L. McNeil, K. J. Kadassery, A. W. McDonagh, W. Zhou, P. Schaffer, J. J. Wilson and C. F. Ramogida, Evaluation of the Effect of Macrocyclic Ring Size on [^{203}Pb]Pb(II) Complex Stability in Pyridyl-Containing Chelators, *Inorg. Chem.*, 2022, **61**, 9638–9649.

44 P. Randhawa, K. J. Kadassery, B. L. McNeil, S. N. MacMillan, L. Wharton, H. Yang, J. J. Wilson and C. F. Ramogida, The H_2S_x macropa Series: Increasing the Chemical Softness of H_2 macropa with Sulfur Atoms to Chelate Radiometals [^{213}Bi]Bi^{3+} and [^{203}Pb]Pb^{2+} for Radiopharmaceutical Applications, *Inorg. Chem.*, 2024, **63**, 21177–21193.

45 M. Tosato, P. Randhawa, L. Lazzari, B. L. McNeil, M. Dalla Tiezza, G. Zanoni, F. Mancin, L. Orian, C. F. Ramogida and V. Di Marco, Tuning the Softness of the Pendant Arms and the Polyazamacrocyclic Backbone to Chelate the ^{203}Pb/ ^{212}Pb Theranostic Pair, *Inorg. Chem.*, 2024, **63**, 1745–1758.

46 J. L. Lange, P. R. W. J. Davey, M. T. Ma, J. M. White, A. Morgenstern, F. Bruchertseifer, P. J. Blower and B. M. Paterson, An octadentate bis(semicarbazone) macrocycle: a potential chelator for lead and bismuth radiopharmaceuticals, *Dalton Transactions*, 2020, **49**, 14962–14974.

47 R. Ferreirós-Martínez, D. Esteban-Gómez, É. Tóth, A. de Blas, C. Platas-Iglesias and T. Rodríguez-Blas, Macrocyclic Receptor Showing Extremely High Sr(II)/Ca(II) and Pb(II)/Ca(II) Selectivities with Potential Application in Chelation Treatment of Metal Intoxication, *Inorg. Chem.*, 2011, **50**, 3772–3784.

48 M. K. Blei, L. Waurick, F. Reissig, K. Kopka, T. Stumpf, B. Drobot, J. Kretzschmar and C. Mamat, Equilibrium Thermodynamics of Macropa Complexes with Selected Metal Isotopes of Radiopharmaceutical Interest, *Inorg. Chem.*, 2023, **62**, 20699–20709.

49 M. Regueiro-Figueroa, J. L. Barriada, A. Pallier, D. Esteban-Gómez, A. de Blas, T. Rodríguez-Blas, É. Tóth and C. Platas-Iglesias, Stabilizing Divalent Europium in Aqueous Solution Using Size-Discrimination and Electrostatic Effects, *Inorg. Chem.*, 2015, **54**, 4940–4952.

50 A. Frei, A. Rigby, T. T. C. Yue, G. Firth, M. T. Ma and N. J. Long, To chelate thallium(i) – synthesis and evaluation of Kryptofix-based chelators for 201Tl, *Dalton Transactions*, 2022, **51**, 9039–9048.

51 A. Roca-Sabio, M. Mato-Iglesias, D. Esteban-Gómez, É. Tóth, A. de Blas, C. Platas-Iglesias and T. Rodríguez-Blas, Macrocyclic Receptor Exhibiting Unprecedented Selectivity for Light Lanthanides, *J. Am. Chem. Soc.*, 2009, **131**, 3331–3341.

52 K. J. KADASSERY and J. J. WILSON, WO/2022/251496, 2022.

53 A. Swidan and C. L. B. Macdonald, Polyether complexes of groups 13 and 14, *Chem. Soc. Rev.*, 2016, **45**, 3883–3915.

54 C. Harriswangler, B. L. McNeil, I. Brandariz, L. Valencia, D. Esteban-Gómez, C. F. Ramogida and C. Platas-Iglesias, Incorporation of Carboxylate Pendant Arms into 18-Membered Macrocycles: Effects on [$^{nat/203}$ Pb]Pb(II) Complexation, *Chemistry – A European Journal*, 2024, **30(28)**, e202400434.

55 J. W. Nugent, H. S. Lee, J. H. Reibenspies and R. D. Hancock, Spectroscopic, structural, and thermodynamic aspects of the stereochemically active lone pair on lead(II): Structure of the lead(II) dota complex, *Polyhedron*, 2015, **91**, 120–127.

56 R. D. Hancock, M. Salim Shaikjee, S. M. Dobson and J. C. A. Boeyens, The Stereochemical activity or non-activity of the 'Inert' pair of electrons on lead(II) in relation to its complex stability and structural properties. Some considerations in ligand design, *Inorganica Chim. Acta*, 1988, **154**, 229–238.

57 N. V. Sidgwick and H. M. Powell, Bakerian Lecture: Stereochemical types and valency groups, *Proc. R. Soc. Lond. A Math. Phys. Sci.*, 1940, **176**, 153–180.

58 L. Shimoni-Livny, J. P. Glusker and C. W. Bock, Lone Pair Functionality in Divalent Lead Compounds, *Inorg. Chem.*, 1998, **37**, 1853–1867.

View Article Online
DOI: 10.1039/D6QI01035K

59 C. Harriswangler, A. Freire-García, S. Argibay-Otero, A. Rodríguez-Rodríguez, J. M. Rodríguez, D. Esteban-Gómez, E. M. Vázquez-López and C. Platas-Iglesias, Structural effects of the Pb^{2+} 6s2 lone pair activity: Eccentricity, *Coord. Chem. Rev.*, 2025, **529**, 216434.

60 H. H. G. Jellinek and J. R. Urwin, Ultraviolet Absorption Spectra and Dissociation Constants of Picolinic, Isonicotinic Acids and their Amides, *J. Phys. Chem.*, 1954, **58**, 548–550.

61 P. Gans, A. Sabatini and A. Vacca, Investigation of equilibria in solution. Determination of equilibrium constants with the HYPERQUAD suite of programs, *Talanta*, 1996, **43**, 1739–1753.

IMPERIAL COLLEGE LONDON
DEPARTMENT OF CHEMISTRY
South Kensington, London SW7 2AZ

Tel: +44 (0)20 7594 5781 FAX: +44 (0)20 7594 5804
E-mail: n.long@imperial.ac.uk
Web site: http://www3.imperial.ac.uk/people/n.long

View Article Online
DOI: 10.1039/D6QI01035K

Professor Nicholas J. Long, FRSC The Sir Edward Frankland BP Chair of Inorganic Chemistry
Royal Society Wolfson Research Merit Award Holder

Data availability statement on "*Picolinamide-functionalized macrocyclic chelators for 203/212Pb theranostic radiotracers"*

I can confirm that all the relevant research data is contained with the manuscript and electronic supporting information. No databases have been used and no references to such databases are contained in the manuscript or ESI.

Best wishes